ICAS-82-3.7.3 # Comparison of HP Turbine "Deep Blade Design" Effects in Turbofan Engine Gas Generators with Different Bearing Structure Configurations

Dr.-Ing. Dieter Rist
Techn. Universität München
Munich, Germany

Abstract

The step from conventional to "deep blade design" (DBD) of a hot gas turbine does not only ensue modifications in blade, root and turbine disk but also in shaft, bearing and force-transferring structures, blade containment elements and other casing parts. For an example a projected turbofan engine with low bypass ratio has been investigated where mainly component parts of the gas generator are concerned. To study the foreseeable quantitative differences two different types of gas generator bearing structure configurations (conceptions B and C) have been considered. The advantages of DBD must be paid for by an increase of engine mass. To estimate this disadvantage the laws of mechanical and thermal similarity can only be applied for some details, because the loads in question are only part of the total load spectrum. Flow, pressure and thermal loads, centrifugal forces, possible unbalances, mass forces due to flight manoeuvres, additional boundary loads near reinforced parts as well as various deformations influence the structural design of the components. Based on mechanical analyses for defined operation and load cases results for mass modifications of the main components are given. Enlarging the HP turbine rotor blade chord length by 50% the mass of the turbofan engine core (HP module) increases for about more than 7% (B) or 11% (C), resp.. This and further results can be used as aids to evaluate some other aspects and effects of HP turbine deep blade design within flight propulsion system studies.

I. Introduction

The tolerable maximum turbine entry temperature of aero gas turbines is limited by various criteria. Since the high pressure turbine (HPT) must run in that very hot gas stream, the blading is one of the most critical component parts. According to investigations on so-called "deep blade design" (DBD), a modern branch within the design philosophies of aero engines, we want to illustrate the influence of this component on the dimensioning of elements, structural members, component parts and modules of the whole engine. The so-called "avalanche effect" due to direct and indirect influences leads to rather differing modification

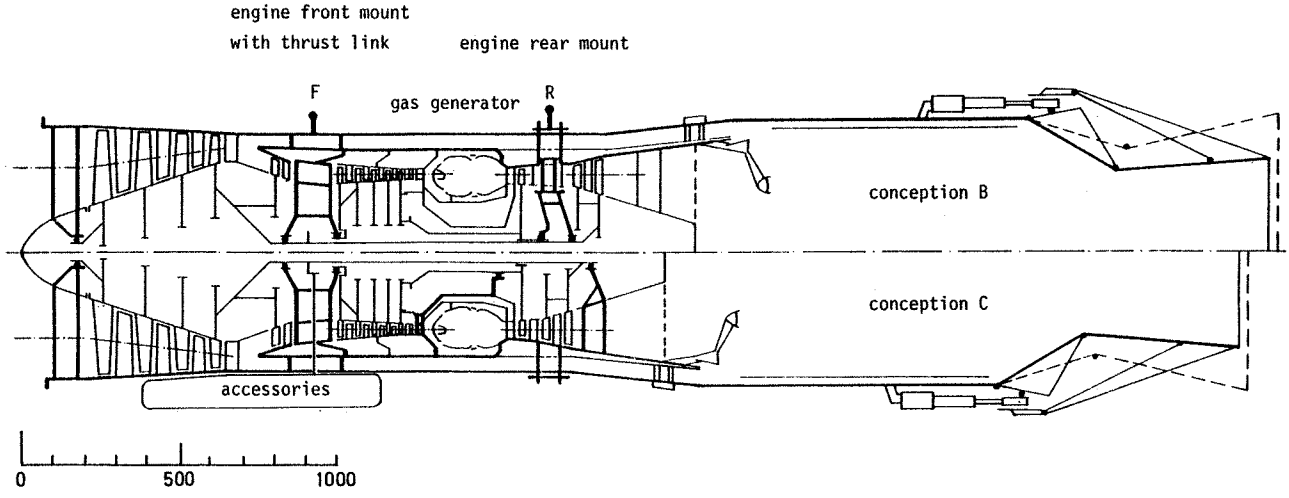

Fig.1: Project of a two-shaft turbofan engine. Bearing structure configurations B and C. True to scale draft.

factors. Owing to the numerous effects of one single variation parameter the large number of further varying facts concerning conception, thermogasdynamic and mechanical design of an aero engine must be fixed for sake of clarity. The example of the investigated typical case with the two different bearing structure configurations shows that many respects of engine design depend on decisions of the engineer demanding an overall view of the consequences.

II. Conception and operation of the aero engine

Engine design

The investigated object is a projected two-shaft turbofan engine with small bypass ratio suitable for supersonic flight. Fig. 1 shows the arrangement of components of the turbofan engine. The low- and medium-pressure turbo machine rotor has a three-fold bearing support and the high pressure turbo machine rotor has a two-fold bearing support. For the effects of HPT modifications it is important where the bearings of the HP rotor are placed. As shown in Fig. 1 two different configurations have been regarded. One of them has the HP turbine in an overhung position (lower part: conception C, "cantilever"), and the other has its bearing supports on both ends of the rotor (upper part: conception B, "beam"). The thrust of the aero engine is transmitted to the aircraft at the front mount F, which is almost directly connected with the front support frame at the compressor side of the HP rotor. The position of the thrust link is one of the values determining the course of the axial load within the structural members. The engine rear mount R is arranged at the HPT exhaust and - in the case of conception B - it is partly integrated with the rear support frame at the turbine side.

The investigations give results with a validity exceeding this special cases because the calculations and considerations on the engine project are based on advanced thermodynamical data and typical component arrangements of supersonic aero engines. The thermogasdynamical main data are listed in table 1. The speeds of the two rotors determine some of the important engine loads, the aerodynamic, centrifugal and gyroscopic forces. The engine size and dimensions may be discerned from the true to scale draft in Fig. 1. Its mass is calculated by use of an estimation procedure[1] with partial corrections by detailed design drafts for gas generator components and by data from known modern engine component parts which were transferred following the principle of mechanical similarity: $M_{Eng} \approx 1150$ kg.

Engine operation

If a fighter aircraft is equipped with the engine in question some of its operation loads are given by the typical flight manoeuvre diagrams shown in Fig. 2. Point H in the flight envelope diagram

			take - off (AP) (ISA 0/0)	high speed flight near the ground (BP)	
air mass flow rate	$\dot{m}_{eng}$	kg/s	100	178	(178%)
bypass ratio	$\dot{\mu}$	-	0.5	0.65	
turbine entry temperature	T_{TE}	K	1800	1800	
reheat temperature	T_{reh}	K	2200	2200	
overall pressure ratio	π_C	-	25	12.9	(51.6%)
low pressure compressor	π_{LPC}	-	4.7		
medium pressure compressor	π_{MPC}	-	1.38		
high pressure compressor	π_{HPC}	-	3.85		
max. against ambient pressure ratio	p_{t4}/p_0	-	25	40	(160%)
HP rotor speed	n_{HP}	rpm	14700	14935	(101.6%)
LP rotor speed	n_{LP}	rpm	12100	10735	(88.7%)
thrust without reheat	F	kN	82.5		
thrust with reheat	F_{reh}	kN	127	174	(137%)

Table 1: Thermogasdynamical data of the projected turbofan engine

indicates the state of a high-speed flight near the ground, where the internal load level is significantly higher than for take-off conditions (ISA 0/0). The operation data under the condition of constant maximum turbine entry temperature ($T_{TE,max}$ = 1800 K) are calculated by use of the engine performance maps which are based on the Mach similarity. The absolute HP rotor speed increases slightly and the LP rotor speed decreases. The overall pressure ratio of the 3 compressors is considerably lower than for take-off condition, but due to stagnation pressure the absolute pressure within the gas generator is higher. Owing to the higher density level the mass flow rates of the entire engine and of the gas generator increase considerably. Some operation data are given in the right column of Tab.1. These data indicate that besides pressure also the axial force loading reaches maximum values for this flight case. Therefore the strength calculations of the most important engine structures must be based on it. Further flight loadings stem from the mass forces due to the aircraft motion. For their estimations the flight manoeuvre load factors as well as the angular velocities and accelerations must be known. The lower diagram in Fig. 2 gives limits of the pitching velocity during curving flights of a fighter aircraft. For the calculation the figures valid for combined loading cases were taken from the MIL specification handbook.[2]

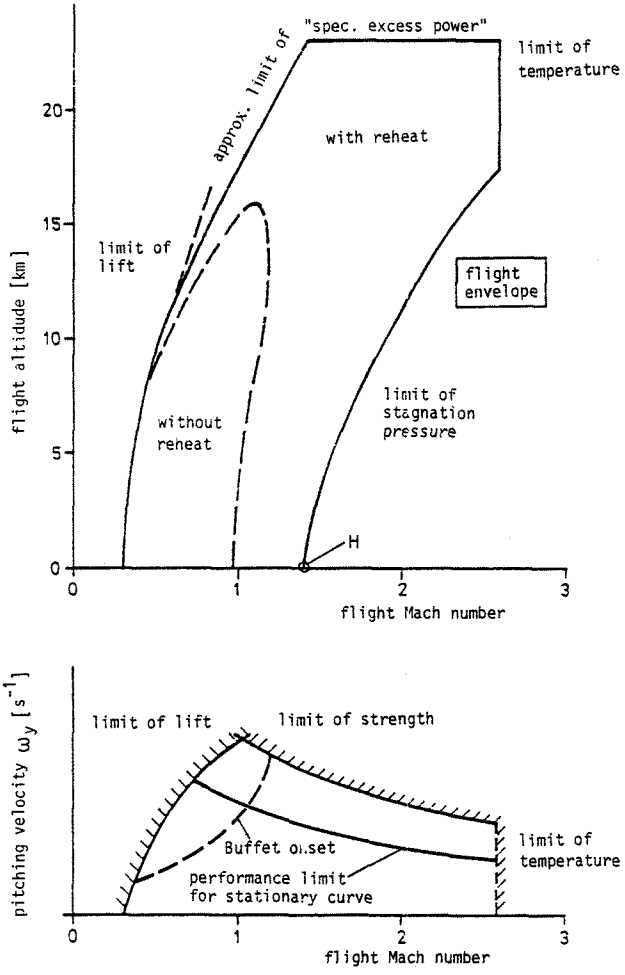

Fig.2: Typical flight manoeuvre diagrams of a modern fighter aircraft

III. Gas generator (HP module)

Fig. 3 shows a true to scale draft of the engine core, the HP module or gas generator, resp.. For comparison, the two bearing structure configurations B and C (dotted lines) are outlined. It is useful to take also the inner bearing support strut of the LP shaft at the support frames of the HP module into design consideration, because the forces of the LP rotor act together with that of the HP rotor on the outer parts of the HP support assemblies.

For a quantitative evaluation a rather detailed thermogasdynamical and technological preliminary design is necessary in order to clarify such problems as air and gas guidance and thermodynamical state (local temperatures and pressures), number of stages, main dimensions, velocities and Mach numbers within the stator and rotor system, arrangement of component parts as well as structure masses and mass distributions. The aero engine is subject to a number of rotationally symmetric loads from

- pressure differences
- axial forces
- torsional moments (torque)
- thermal forces
- centrifugal forces (rotor) and

non-rotationally symmetric (asymmetric) loads from

- flight manoeuvre load factor
- gyroscopic effects and
- unbalance.

The loads have their corresponding deformations. The first three rotationally symmetric loads do not change when the HPT rotor blade chord length is enlarged. For modifications of the bucket only the centrifugal forces (from the first group) have

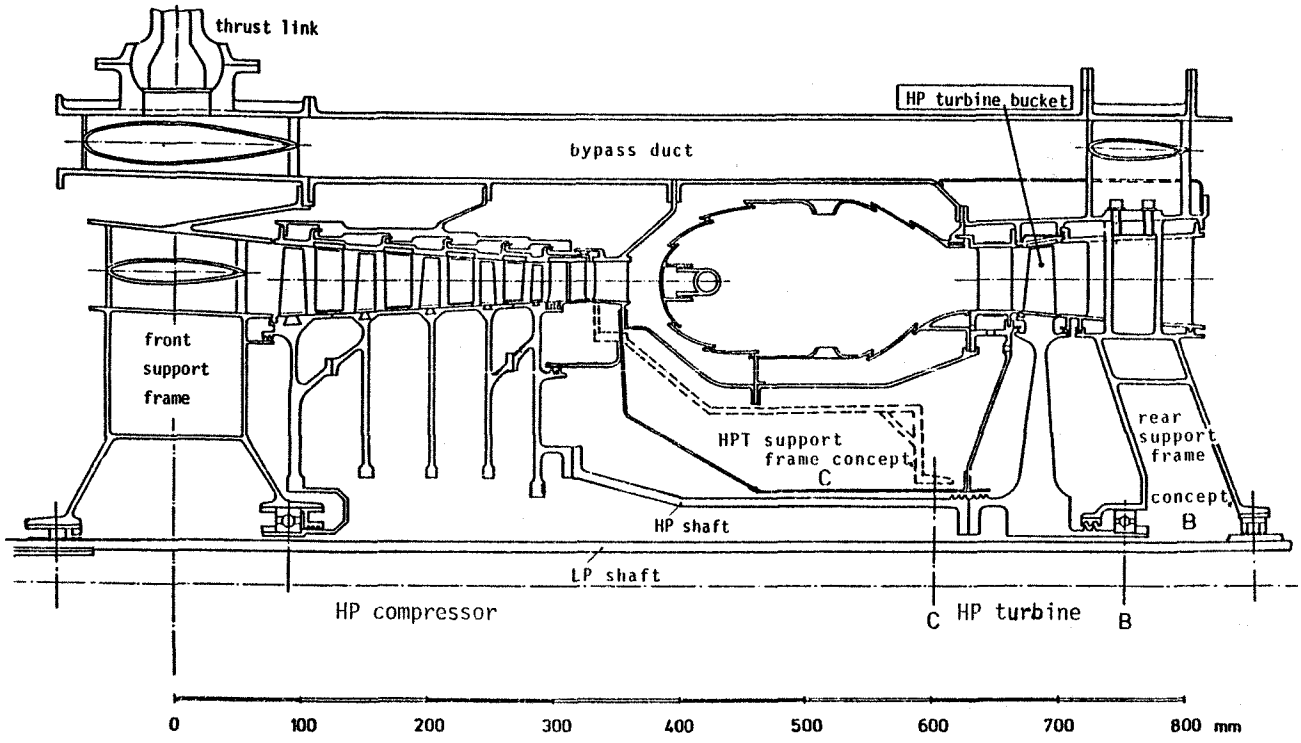

Fig.3: Gas generator (HP module) of the projected two-shaft turbofan engine. HPT bearing structure configurations B and C. True to scale draft.

a direct and considerable influence on the shape of the turbine rotor. With constant stress level and stationary engine operation conditions the radial deformation may be kept constant. Yet with transient operation conditions the temperature state of the thicker rotor changes slower. This fact has to be considered for the shaping of the casing wall within the turbine section.
Within the overall loading the asymmetric loads are almost neglectable because of their order of magnitude. Still the deformations must be considered separately because of their asymmetry. Since this group of loads consists only of mass forces variations of component parts (causing no performance changes) have a greater influence on the load and deformation values.

A survey of effects on mass and dimensions of engine elements and components caused by the variation of the HP turbine bucket chord length is given in Fig. 4. There are influences on various items: axial length, structure load and stress, non-axially symmetric deformations due to mass forces, vibration characteristics and rigidity of support, damage control or blade containment ability, resp., transient thermal extension, heat transfer, manufacturing aspects and others. Some of the engine elements are directly influenced by DBD, others indirectly and a third category not at all.

High pressure rotor

Turbine rotor

Fig. 5 shows on the left a turbine rotor with conventional blading and on the right the change in shape for the deep blade design (DBD).
Bucket aerofoils:
We assume that the wall thickness of the hollow blades remains constant when varying this component element.An enlargement of the chord length and the blade profile modified according to the similarity principle ensues the following advantages:

- Lower mechanical stresses and strains resulting from gas bending forces. Decrease of deflection and bending stresses due to the larger areal moment of inertia and moment of resistance of the profiles. (Vibration stresses must be considered separately.)
- Lower thermal stresses and strains. Decrease of the outer heat transfer and thermo stresses by changing the Nusselt and Biot numbers. (For reasons of heat transfer to the cooling air it is not suitable to apply exactly the rules of geometrical similarity to the inner skeleton of the blade profile.)

- Better resistance against erosion and foreign object damage (FOD).
- Less component parts (blades and fittings),
- Higher allowable manufacturing tolerances at the buckets.
- Lower performance decrease with rising operation time.

The first two items give rise to expectations for a longer life and better reliability. Under certain circumstances possible disadvantages are an increase of vibration stresses and a slight decrease in the HP turbine efficiency. Yet there are measures to keep both effects neglectable. The second one may be avoided by keeping the aspect ratio h/c within certain limitations.[3]

Due to the constant wall thickness and constant blade height the mass of a single bucket aerofoil alters almost linear-proportionally to λ: $M_{aerofoil} \sim \lambda^{1.08}$. Since the number of blades decreases inversely proportional to λ the mass of all bucket aerofoils remains almost constant (see Fig. 10).

Bucket roots:

This bucket element consists of a base plate, an extension part and a fir tree root. The calculation of the main dimensions follows a system of equations incorporating 5 criteria: Tensile stress and heat transfer at the extension part, tensile stress at the first cross section between the root serrations, shear stress at the serrations and tensile stress at the dead rim.[4] The mass of the total blading changes according to the comprehensive approximative formula

$$M_{blading} \sim 1+0.92\cdot(\lambda-1)^{1.17} \quad \text{for } 1 \leq \lambda \leq 2 \qquad (1)$$

HP turbine rotor:

On the right of Fig. 5 the modification of the complete turbine rotor is shown. The centrifugal forces of the blading and the dead rim act as radial outer ring load at the disk. The external load increase necessitates an enlargement of the disk profiles as shown in the figure. Accordingly the approximate change of the turbine rotor mass is

$$M_{HPT\ rotor} \sim 1+0.58(\lambda-1)^{1.09} \qquad (2)$$

+...advantageous aspect of DBD
d...direct significant effect
l...little effect
0...neglectable or no influence

				geometry (axial lengthening)		load and stress modification		deformation due to non-rot. symmetric loads		vibration characteristics (natural frequencies, elasticity of support et al.)		mechanical energy (damage, blade containment)		thermal energy (change of radial clearance in operation)		manufacturing influences, heat transfer and other aspects	
			conception	B	C	B	C	B	C	B	C	B	C	B	C	B	C
gas generator rotor assembly	HPT rotor	HPT bucket	single HPT rotor blade (aerofoil)	d	d	+	+	0	0	d	d	+	+	l	l	+	+
			single HPT blade root	d	d	d	d	0	0	d	d	d	d	l	l	d;+	d;+
			HPT rotor disk	d	d	d	d	0	0	d	d	0	0	d	d	l	l
			HP rotor shaft	l	l	l	l	d	d	d	d	0	0	0	0	0	0
			HP compressor rotor	0	0	0	0	0	0	0	0	0	0	l	l	0	0
			bearings	0	0	d	d	0	0	0	0	0	0	0	0	0	0
gas generator stator assembly	bearing support frames and engine mounting		HP-compressor bearing support frame (flanges, shells, struts)	0	0	(l)	(l)	l	l	(l)	(l)	0	0	0	0	0	0
			HP turbine bearing support frame	0	l	l	l	l	d	l	d	0	0	0	0	0	0
	HP turbine stator assembly incl. blade containment elements			d	d	0	(l)	(l)	l	(l)	(l)	d	d	d	d	l	l
	combustor section			0	0	0	0	0	0	0	0	0	0	0	0	0	0
	HP compressor stator assembly			0	0	0	0	0	0	0	0	0	0	0	0	0	0
	load carrying structure of gas generator casing assembly			d	d	(l)	(l)	(l)	l	(l)	(l)	0	0	0	0	0	0
load carrying structure of engine casing assembly incl. bypass duct casing				l	l	0	0	0	0	(l)	(l)	0	0	0	0	0	0

conception B : HP rotor supported at both outside ends
conception C : HP turbine in overhung position (cantilever)

Fig.4: Matrix of influences on mass and dimensions caused by the variation of the HP turbine rotor blade chord length.

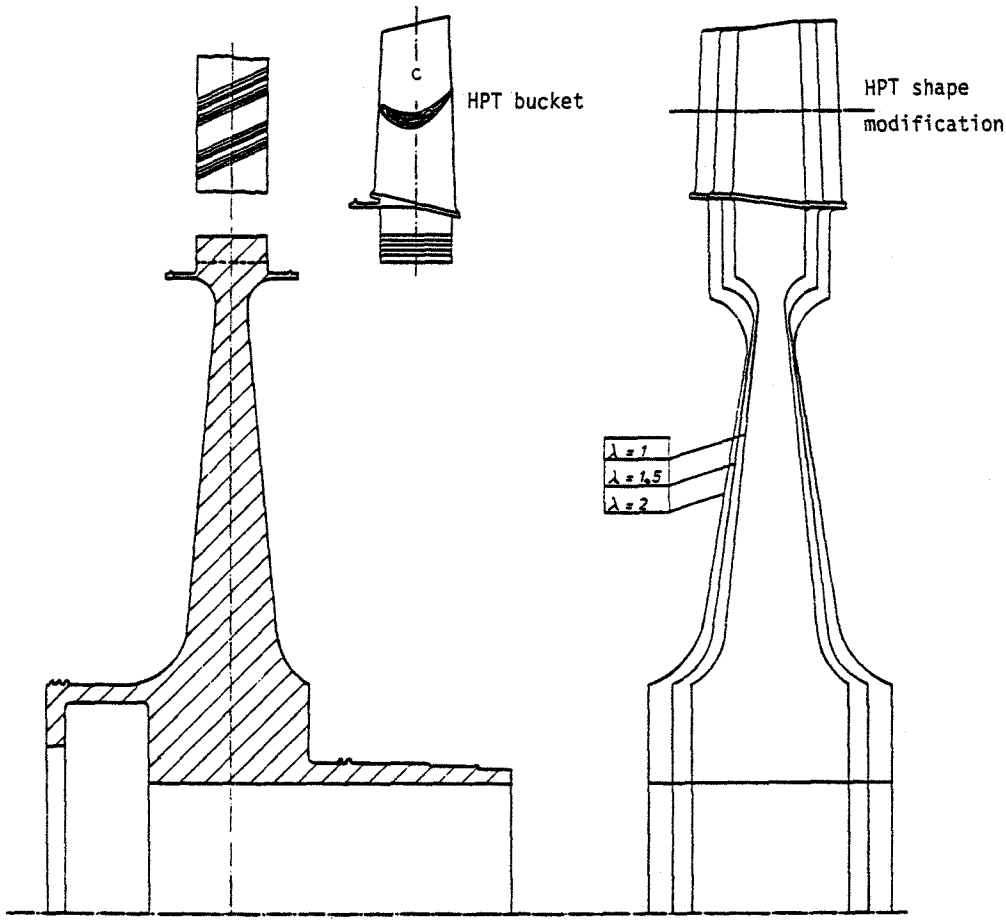

Fig.5: Rotor of the high pressure turbine.
Modification of the shape caused by variation of the blade chord length.

Entire rotor

As to be seen in Fig. 6, the entire rotor consists of the HP compressor, HP shaft and HP turbine rotor. For bearing configuration B in that figure the internal shear forces and bending moments, stemming from the asymmetric loads, for λ=1(CBD) and λ=2(DBD) are outlined along the rotor axis. Especially the notched lines of the bending moments of the gyroscopic load indicate that the rather continuously distributed loads have been introduced into the calculation as comprehensive discrete values. These values as well as that of the flight manoeuvre load factor are computed according to the MIL standard, for ω_y=1.4 rad/sec and n=10, resp.. The assumed unbalance load corresponds approximately to a missing turbine bucket aerofoil. The lines of the axial forces and torsional moment (torque) drawn below with ten-fold scales indicate that the rotationally symmetric loads ($F_{centr.}$; F_{ax}; Δp, M_t, ΔTemp.) are practically independent of λ. They are by about one order of magnitude larger than the λ-dependent asymmetric loads. By the design, fixing of the inner cooling and blocking air guidance and arrangement of the sealing elements, the distribution of axial forces acting at the rotor gives a resultant force in forward direction which acts on the thrust bearing at the HP compressor side.

In Fig. 7 different effects of the bearing configurations B and C on the internal loads can be recognized. There are no great differences of value at the rotor, but the signs are partly opposite. The upper two loads, standing exactly perpendicular to each other, are alternating with high frequency (depending on the rotor speed). The load from the assumed turbine unbalance is a stationary one for the rotor. From the course of the shear forces we can read the bearing forces at the appropriate positions which act on the support frames.

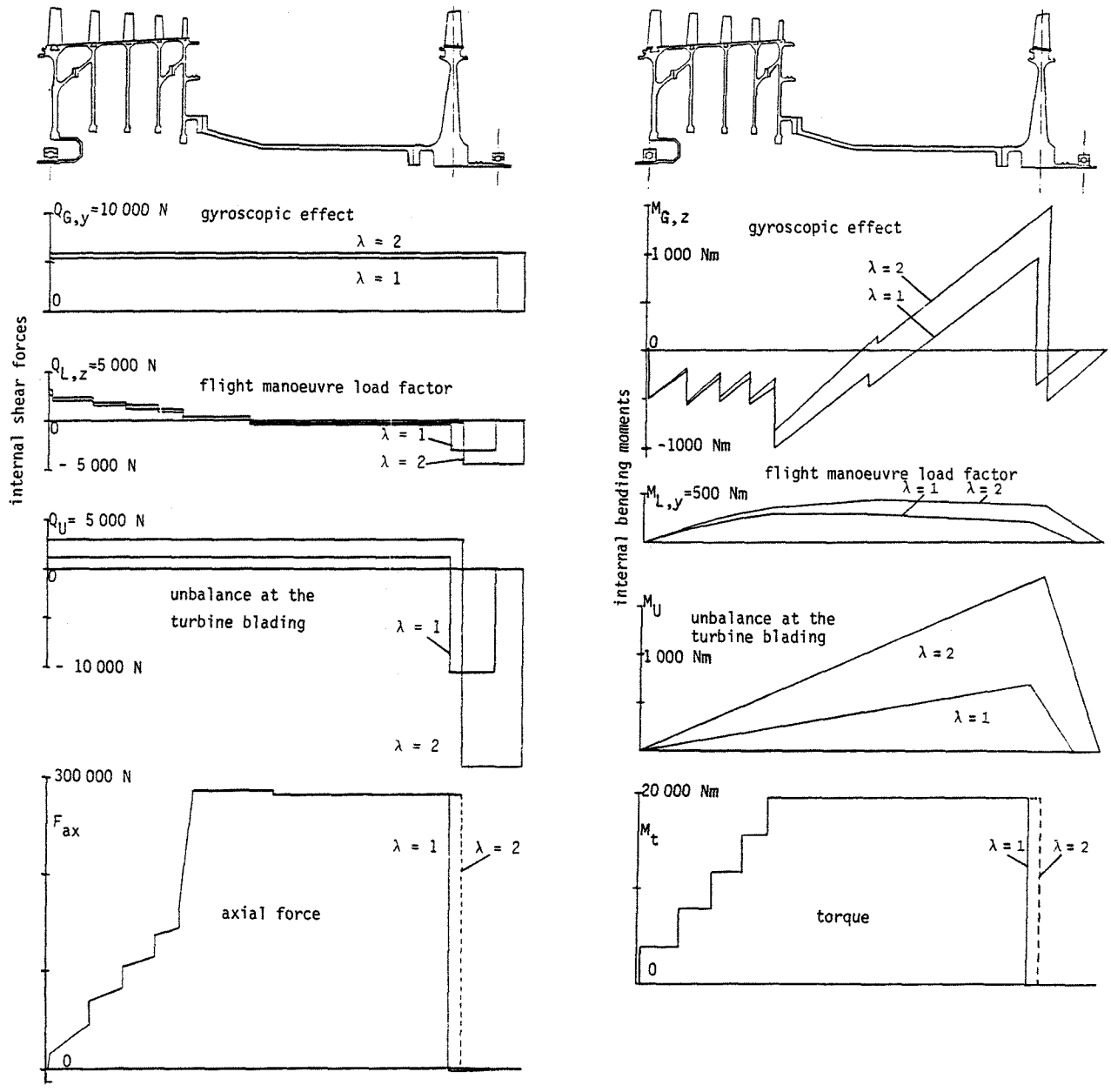

Fig.6: High pressure rotor, bearing conception B.
Above: Internal loads from mass forces altered by variation of the turbine blading.
Below: Axial forces and torsional moment under operating condition "high-speed flight near the ground".

The dimensioning of the rotor according to the strength safety factor leads to hardly any modifications of other components (compressor, shaft) accompanying the turbine variation, since the asymmetric loads only play a minor role within the total load collective. Yet the values of the asymmetric deformation contributions are too high to be neglected. Fig. 8 shows the deflection of the rotor (bearing configuration B) for λ = 1(CBD) and λ = 2(DBD) where generally the shear deformation amounts to about 20% to 25% (30% at the most) of the bending deflection. The dotted lines in Fig. 8 demonstrate that the static deformation of the shaft caused by the unbalance at the turbine side is the main contribution to the resulting deflection. In the case of λ = 2(DBD) the maximum deflection exceeds 0.2 mm, and therefore the rotor must be reinforced at certain positions. To establish a tendency only deformation caused by unbalance may be considered. A simple conversion of all three influences is not possible,

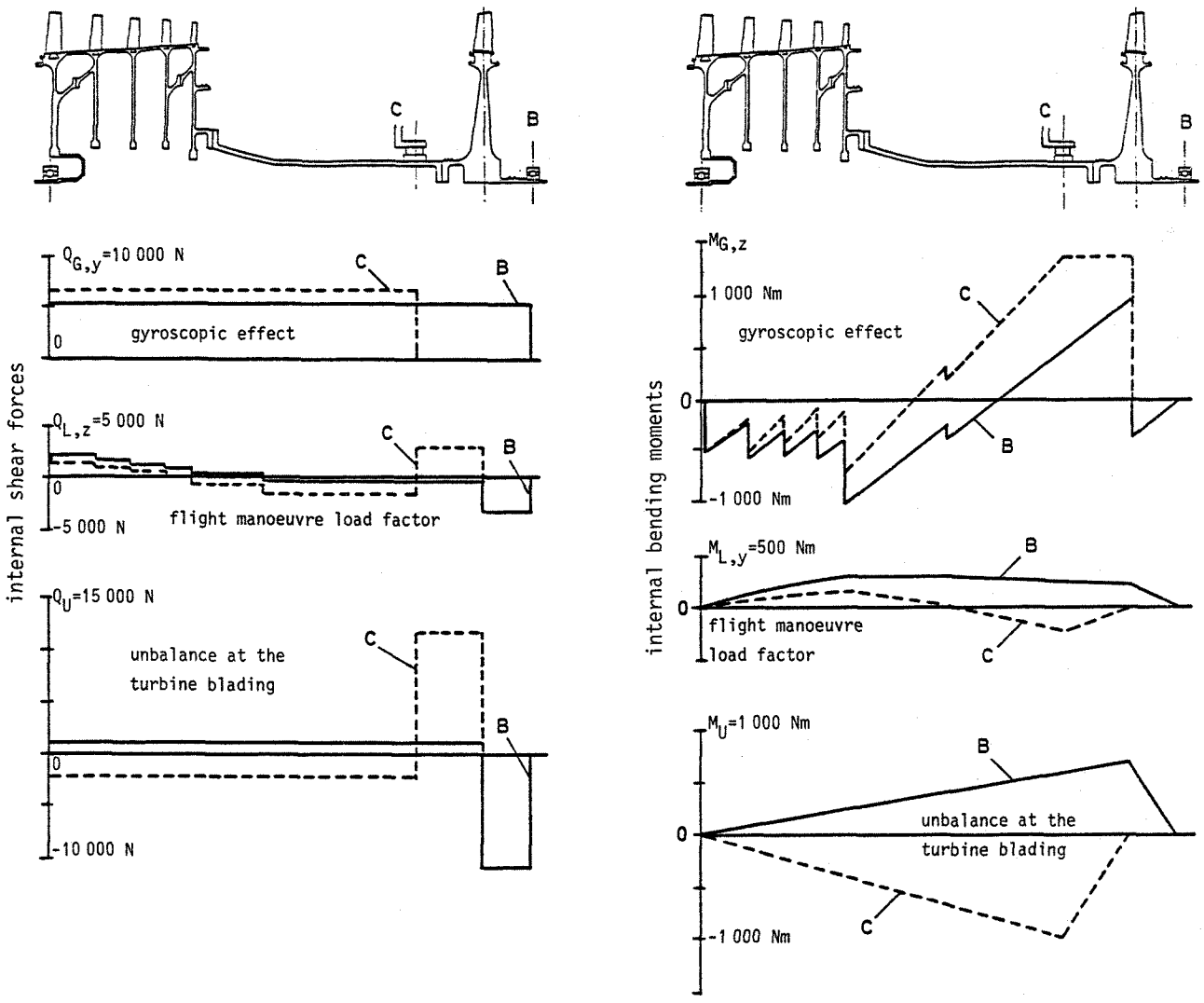

Fig.7: High pressure rotor, turbine with "conventional blade design, CBD". Internal loads from mass forces altered by variation of the bearing structure configurations (conceptions B and C).

since for instance the deformation shape caused by gyroscopic effects changes. To lower the deflection it is sufficient to enlarge only the areal moment of inertia of the hollow shaft, because the very stiff disk-drum rotor of the HP compressor is hardly deformed. In order to combine the two criteria "allowable stress" and "allowable deflection" for the hollow shaft, being optimized with respect to weight, a compromise between cross section area and areal moment of inertia must be found. The chain-dotted curve in Fig. 8 shows that the deflection for λ = 2(DBD) may keep approximately the same value as for λ = 1(CBD) when doubling the areal moment of inertia of the shaft.

Lower critical rotor speeds follow mainly from the increased axial lengths and bearing distances, whereas the greater masses and wall thicknesses have only little influence in that respect. Fig. 9 shows that the alterations due to the turbine variation for the case of bearing conception C are larger than for the case of conception B.

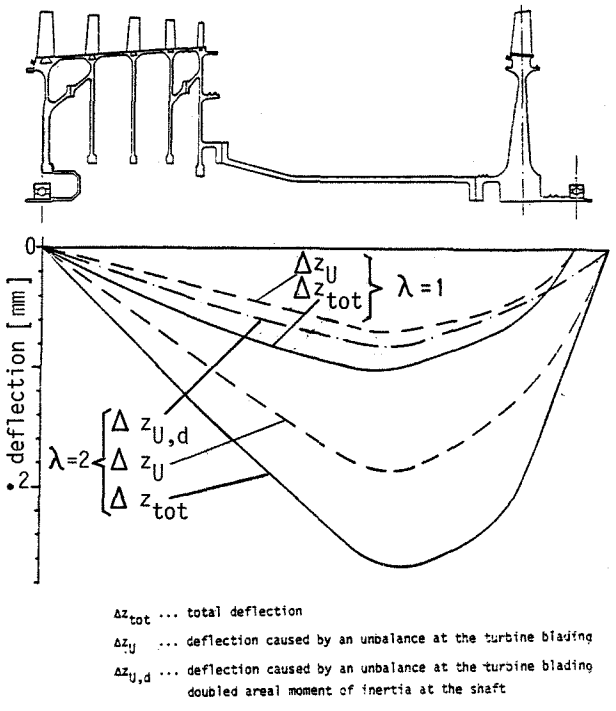

Fig.8: High pressure rotor,bearing configuration B. Deflection from mass forces changed by variation of the turbine blading .

Bearing support frames

As shown in Fig. 3 the bearing support frames at the compressor and turbine side of the HP module are assembled of cylindrical and conical support shells and liners, struts, mounts and brackets. Besides their supporting function, they are also used as lead through for the accessory drive (front support frame, see Fig. 1), bleed air guidance, lubricating oil supply, etc.. Their main dimensions are chosen according to strength considerations (pressures, axial forces), and the resulting relatively large hollow profiles of the struts are useful for the secondary purposes just mentioned. The total deformation stemming from the asymmetric load is composed of many single deformations and we have to consider it seperately as criterium for the dimensioning of the wall thickness. At one of the strut sections for instance there occur extension/compression as well as bending deflection and shear deformation of the struts and additionally elongation/shortening of the casing liner part. Towards the outer parts of the support frames the load factor becomes gradually more important since by and by the stator mass forces of the gas generator and finally those of the complete turbofan engine are added. Accordingly the percentage of influence of the turbine variation on the supporting elements changes. Since the structures are thin-walled the deformation may be kept approximately constant by modifying the wall-thickness proportionally to the overall load changing. For most structural elements a linear relation between load and geometry may be applied with sufficient accuracy for regions outside the influence of stiffeners (characteristic Wagner value).

Although the deformation of the front support frame is influenced by the HP turbine variation there is no need for stiffening the structure because the deformation is small enough. Contrary to that the elasticity of the rear support frame of both conceptions, B and C, is important in any case. As to be seen in Fig. 9, certain rigidities of support are necessary to hold a specified security distance between the first critical and the rotor operation speed. Especially the turbine support frame C must be reinforced for that reason when λ is greater than 1. Another reason is the bearing displacement which already in the original design case (λ=1) is about 0,2 mm and ought not to enlarge.

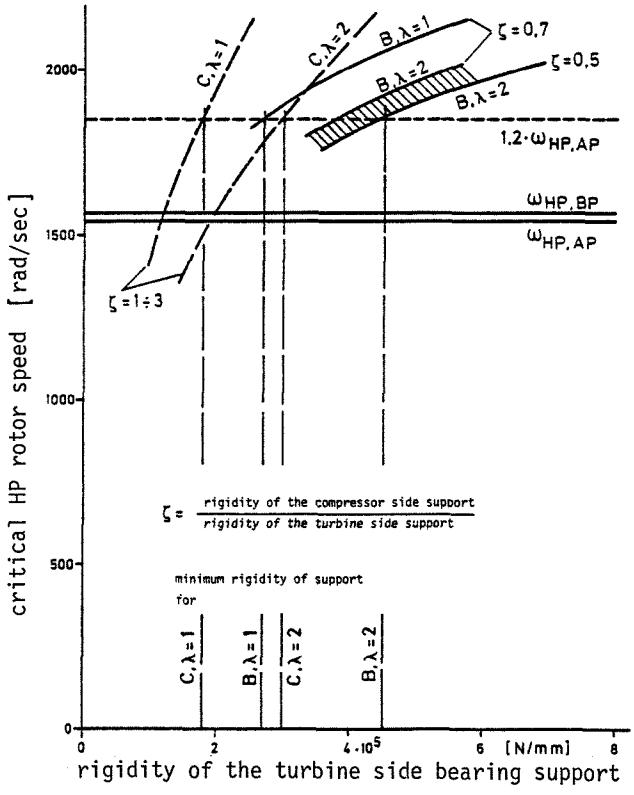

Fig.9: First critical rotor speed in dependance of the rigidity of support. Effects of bearing structure configurations (conceptions B and C) and turbine variation (λ =1 and 2).

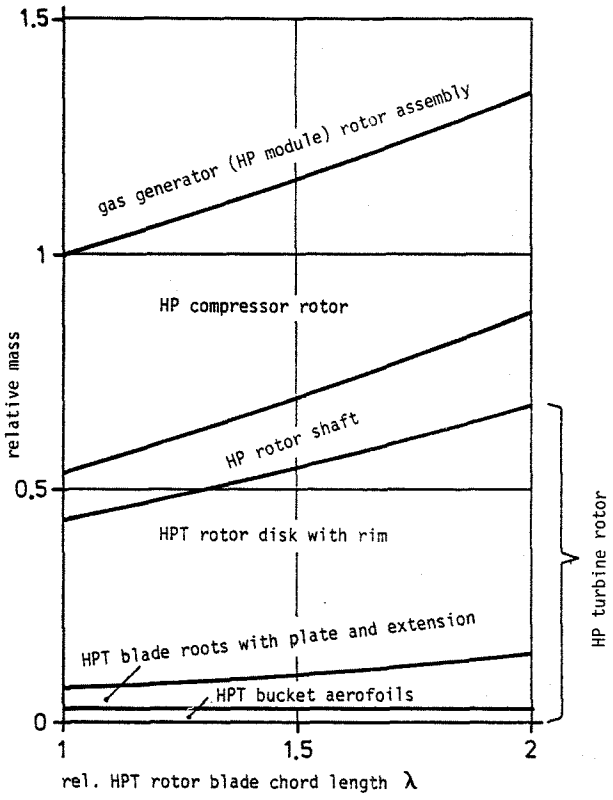

Fig.10: High pressure rotor
Increase of the total mass and mass fraction rates with enlargement of the HP turbine rotor blade chord length.

Gas generator stator and casing assembly

As the HP turbine stator assembly also the bypass casing liner of this section is affected by the axial lengthening caused by the HPT bucket variation. The inner turbine casing liner has a function as flow guidance and furthermore its dimensions are designed for blade containment ability and transient thermal expansion adapted to that of the turbine rotor. An analysis of various reports and empiric formulae concerning blade containment yield the following relation between casing wall-thickness and mass fragments[5]:

$$t \sim M_{fragment}^{n} \quad \text{with } n = 1/3 \ldots 2/3$$

In our damage case $M_{fragment}$ is represented by the mass of one bucket. This gives a direct correlation with the variation of the HPT bucket. Since the elasticity and deformation is relatively small no further modification must occur at the load carrying casing structure nor within the section of combustor and HP compressor stator.

IV. Mass modification

Fig. 10 shows the relative increase of the HP rotor mass when lengthening the HPT bucket profile chord. The differences between conception B and conception C are too small to be outlined. On the contrary the differences are significantly higher for the entire HP module, see Fig. 11. The 7 criteria of dimensioning, named in Fig. 4, result in minimum and maximum mass modifications which are marked by the full and dotted lines, resp.. The corresponding formulae are

$$(M/M_{CBD})_{HPRotor} \approx 1+0{,}34\cdot(\lambda-1)^{1.05} \qquad (3)$$

$$(M/M_{CBD})_{HPModule} \approx 1+k_{HPM}\cdot(\lambda-1) \qquad (4)$$

$$M_{CBD,HPModule} \approx 0.19\cdot M_{Eng} \quad \text{for conc. B}$$

$$\approx 0.175\cdot M_{Eng} \quad \text{for conc. C}$$

$$k_{HPM} \approx 0.14 \ldots 0.19 \quad \text{for conc. B}$$

$$\approx 0.22 \ldots 0.40 \quad \text{for conc. C}$$

$$(M/M_{CBD})_{Engine} \approx 1+k_{E}\cdot(\lambda-1) \qquad (5)$$

$$k_{E} \approx 0.027 \ldots 0.037 \quad \text{for conc. B}$$

$$\approx 0.038 \ldots 0.069 \quad \text{for conc. C}$$

A 50% increase of HPT bucket chord lenght for case B entails mass enlargements of more than 7% for the HP module and 1.4% for the complete engine, whereas for case C we get more than 11% and 1.9%, resp.. These results, compared with the DBD advantages, make clear that recommendations can only be given if the entire task and operation program of the aero engine is known.

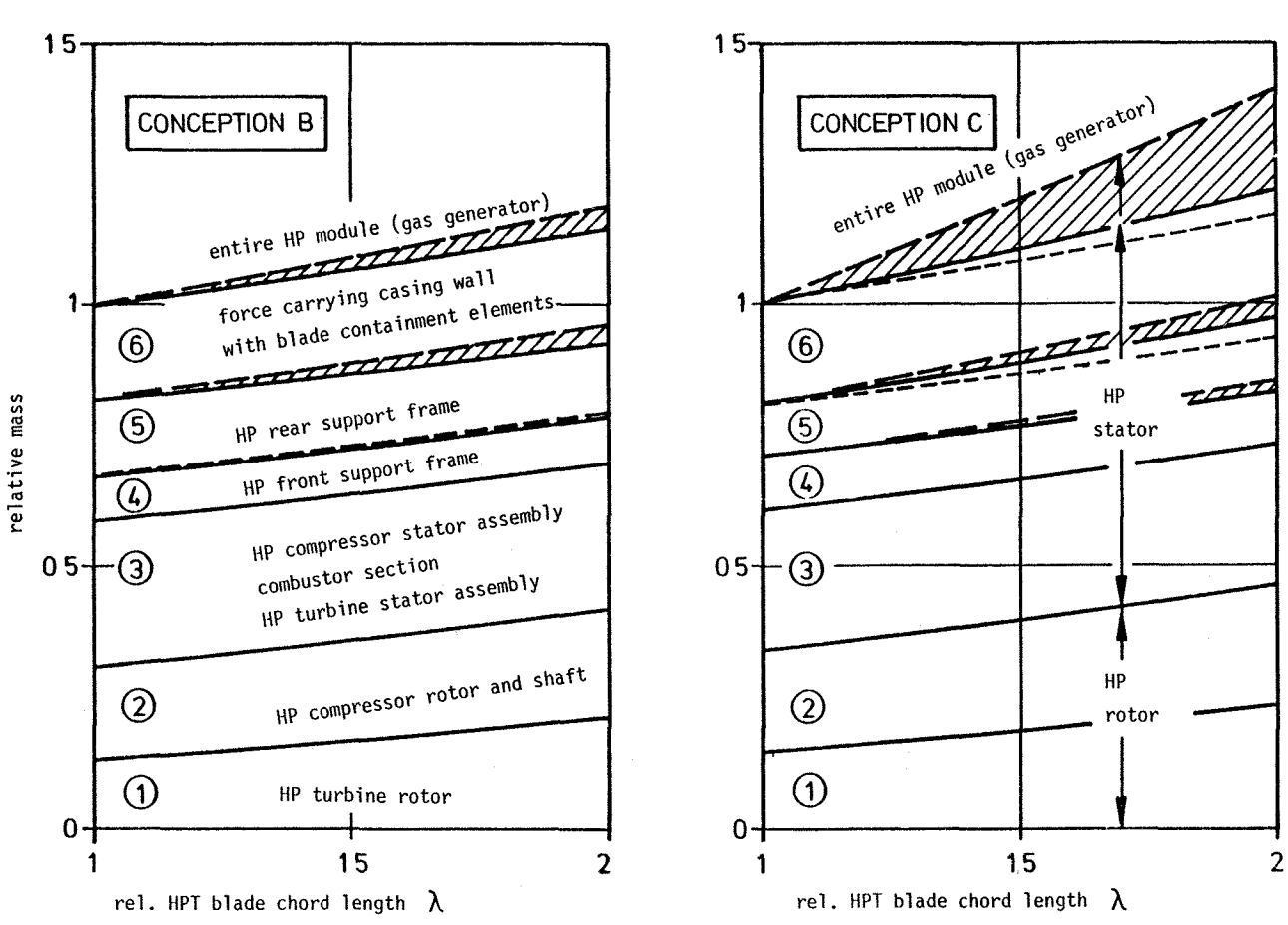

Fig.11: High pressure module (gas generator) of the projected turbofan engine.
Increase of the total mass and mass fraction rates with enlargement of the HP turbine rotor blade chord length.
Influences of the bearing structure configuration (conceptions B and C) and of other criteria.

References

(1) Klees G.W.; Fishbach L.W. : Aircraft Engine Weight Estimation Method. 37th Ann. Conf. of the Soc. of Allied Weight Engineers. Munich/W.Germany, May 1978

(2) : Military Specification Engines, Aircraft, Turbojet and Turbofan MIL - E - 5007 D.

(3) Rist D. : Influence of Geometric Effects on the Aspect Ratio Optimization of Axial Turbine Bladings. ASME-publication 78-GT-173, April 1978

(4) Rist D. : Zur thermogasdynamischen und technologischen Auslegungsphilosophie komplexer Turbostrahltriebwerke Bericht des Lehrst. f. Flugantriebe, Tech. Universität München, Mai 1982

(5) : Advances in Engine Burst Containment and Finite Element Application to Battle-Damaged Structure AGARD-Rep. R-648, Sept. 1976